Large-Area Flexible Ultrasonic Imaging System With an Organic Transistor Active Matrix

Yusaku Kato, *Student Member, IEEE*, Tsuyoshi Sekitani, Yoshiaki Noguchi, Tomoyuki Yokota, Makoto Takamiya, *Member, IEEE*, Takayasu Sakurai, *Fellow, IEEE*, and Takao Someya, *Member, IEEE*

Abstract—We have successfully fabricated a large-area flexible ultrasonic imaging system by integrating a polymeric ultrasonic-transducer array sheet with an active matrix of organic field-effect transistors. The ultrasonic sheet comprises 8×8 ultrasonic sensing cells with an effective size of 25×25 cm^2. The organic transistors exhibit mobility of 0.1 and 0.5 cm^2/V · s at the low operation voltage of 1 mV and in the saturation regime, respectively. When an ac signal is applied between source and drain electrodes for the transistors with a grounded gate, the on/off ratio is larger than 10^4 at the carrier frequency of 40 kHz. In the linear sensing array comprising eight ultrasonic cells, crosstalk is suppressed sufficiently low, and the on/off ratio exceeds 10^4. Images in free space are obtained for multiple-target objects over this sheet.

Index Terms—Large-area sensor, organic transistor, polyvinylidene fluoride (PVDF), ultrasonic wave.

I. INTRODUCTION

ORGANIC FETs [1]–[5] are suitable for large-area flexible electronics since organic transistors can be fabricated on a plastic substrate at an ambient and/or low temperature by using printing processes. In the past decade, utilizing these advantages, various types of novel applications have been proposed and demonstrated. In particular, applications such as flexible displays [6]–[8] and RF identification (RFID) tags [9]–[11] have attracted considerable attention. In addition to these applications, large-area sensors and actuators are expected to open up a new class of large-area electronics. Recently, many large-area devices such as large-area gas sensors [12], [13], pressure and temperature sensors [14], [15], sheet-type scanners [16], large-area actuators [17], wireless power transmission sheets [18], and wireless communication sheets [19] have been reported.
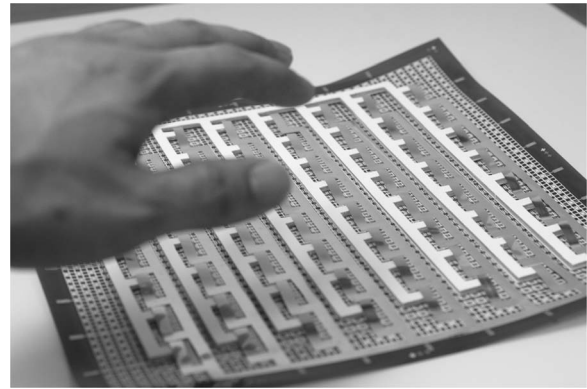
Fig. 1. Image of an ultrasonic imaging sheet comprising an 8×8 array of ultrasonic sensing cells. The sensing cells are formed by integrating a printed organic transistor sheet and an ultrasonic transducer array sheet. This system is mechanically flexible and can be wrapped around a robot's body.

We have recently reported, at an IEEE International Electronic Devices Meeting [20], a successful fabrication of a large-area flexible ultrasonic 3-D imaging system by integrating an ultrasonic-transducer array sheet, which is made of a polymer piezoelectric material, with an active matrix of printed organic FETs. In this paper, we report a systematic characterization of ultrasonic sensor sheets and provide considerable technical details of the device fabrication process. The proposed system comprises 8×8 ultrasonic sensing cells or others and has a printed area of 25×25 cm^2. The printed transistors ($\mu_{\text{saturation}} \sim 0.5$ cm^2/V · s) with a grounded gate can switch 40-kHz signals with an on/off ratio of $> 10^4$. Three-dimensional ultrasonic images can be obtained for multiple-target objects over this sheet. This system can detect target objects behind a cloth and a paper. It is mechanically flexible and can be wrapped around a cylindrical bar, as shown in Fig. 1; this configuration is suitable for obtaining a viewing angle of $360°$ for a medium-length (about several meters) proximity robotic skinlike sensor.

II. MATERIALS AND MANUFACTURING PROCESS

The ultrasonic sensing cell comprises one organic transistor and one ultrasonic transducer. The cross-sectional illustration of an ultrasonic sensing cell is shown in Fig. 2. A transistor active-matrix sheet and an ultrasonic-transducer array sheet (Fig. 3) are separately manufactured and then electrically connected to each other. The circuit diagram is shown in Fig. 4. One side of the transducer is connected to the drain of the transistor.
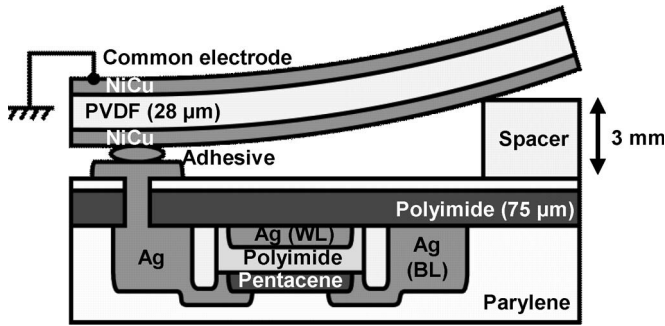
Fig. 2. Cross-sectional view of an ultrasonic sensing cell. An organic transistor active matrix is laminated with an array of ultrasonic transducers using a silver paste. The ultrasonic transducers are bent by the spacer to improve sensitivity. The transducer and spacer sheets are patterned to produce the pixel structure using a numerically controlled cutting system.
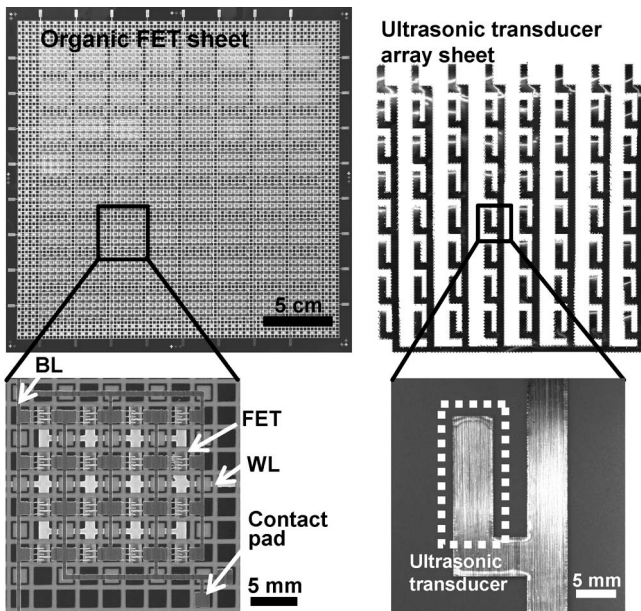

Fig. 3. Photographs of the ultrasonic imaging sheet. The sensing cells are spaced by intervals of 1 in. To achieve a low channel resistance, 16 transistors are connected in parallel. The dimensions of the ultrasonic transducer are 5 mm × 10 mm $(W \times L)$; the transducer is patterned using a numerically controlled cutting system.
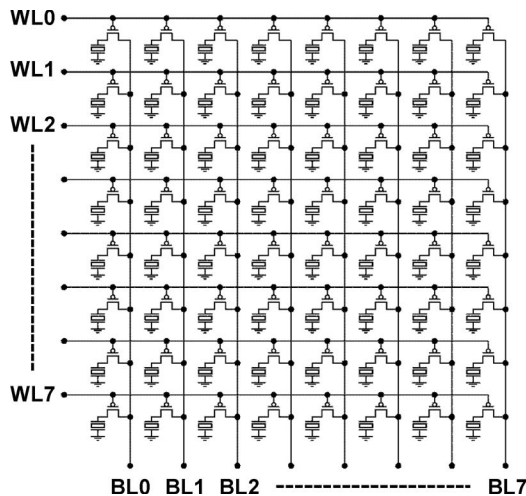

Fig. 4. Circuit diagram. Each sensing cell has one ultrasonic transducer and one transistor.

A. Printed Organic Transistor Active Matrix

The organic transistors with top-contact geometry are fabricated on a 75-μm-thick polyimide film. Compared with the organic transistors with bottom-contact geometry, the organic transistors with top-contact geometry show relatively small contact resistance [21]; this is suitable for small-signal operations of devices such as ultrasonic devices. First, a gate electrode is deposited on the substrate film by inkjet printing or vacuum evaporation. As a gate dielectric layer, a 500-nm-thick layer of polyimide (CT4112, Kyocera Chemical Corporation) is formed by inkjet printing or spin coating and cured in a clean oven at 180 °C for 1 h. Then, a 50-nm-thick pentacene channel layer is deposited by vacuum evaporation using a printed shadow mask [22]. Finally, source and drain electrodes are formed by inkjet printing or vacuum evaporation. The manufactured transistor matrix is encapsulated within a 5-μm-thick layer of parylene (Daisan Kasei, Ltd., diX-SR) by using chemical vapor deposition. Regardless of manufacturing processes, printing, or vacuum evaporation, transistor performances are almost the same; however, yields of vacuum-evaporated transistors are higher than those of printed transistors. Therefore, in the following, we used organic transistors manufactured using vacuum evaporation, unless otherwise noted.

B. Ultrasonic-Transducer Array Sheet

A 28-μm-thick piezoelectric polyvinylidene fluoride (PVDF) film whose surfaces are covered by NiCu is used as a sheet-type ultrasonic transducer. Although the piezoelectricity of PVDF is smaller than that of lead zirconate titanate (PZT), PVDF has many advantages with respect to its application to an ultrasonic imaging sheet, such as mechanical flexibility, light weight, low cost, compatibility to large-area manufacturing in sheet-type transducers, low acoustic impedance (compatibility to air-range transducer), and a small resonance Q value that is required for obtaining a narrow pulsewidth. Since position sensing is explored in free space, the frequency of the ultrasonic wave is adjusted to be 40 kHz to avoid significant attenuation.[1] The transducers are used in the transverse mode (d_{31} mode) to set the resonance frequency to 40 kHz. The resonance frequency of the ultrasonic transducer in the d_{31} mode can be controlled by changing the bending radius of the transducer [23], [24]. In this device, one side of the transducer is attached to the substrate, whereas the other side is kept as a free end and lifted by a spacer sheet to improve the sensitivity at 40 kHz. This bending structure is easy to fabricate in sheet-type and large-area devices. The manufactured transducers can be used as both receivers and transmitters without any change in their structure.

III. DEVICE CHARACTERISTICS

A. High-Speed Printed Organic FETs

Stand-alone organic transistors are characterized. All the measurements are carried out in ambient air. First, we measure

---

[1]We should consider attenuation of ultrasonic wave in free space for air-coupled application. Attenuation of ultrasonic wave is proportional to the square of its frequency.
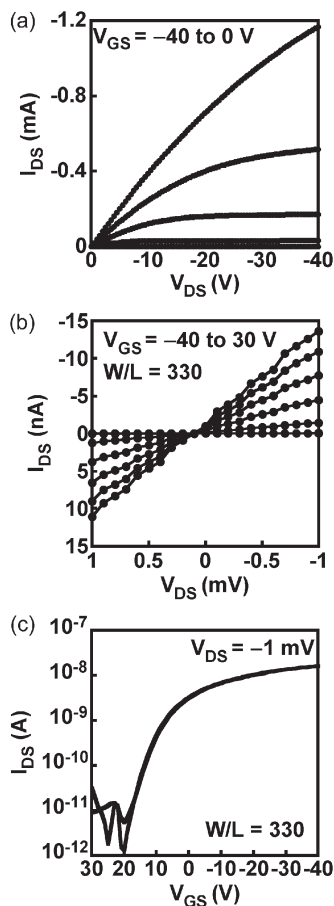
Fig. 5. Small-signal operation of organic FETs. (a) Plot of the source–drain current I_{DS} versus the source–drain voltage V_{DS}. (b) Operation of the organic FETs with a small V_{DS} value. A plot of I_{DS} versus V_{DS} in a linear regime. (c) I_{DS} versus gate–source voltage V_{GS} of the organic transistors in a linear regime ($V_{DS} = -1$ mV).
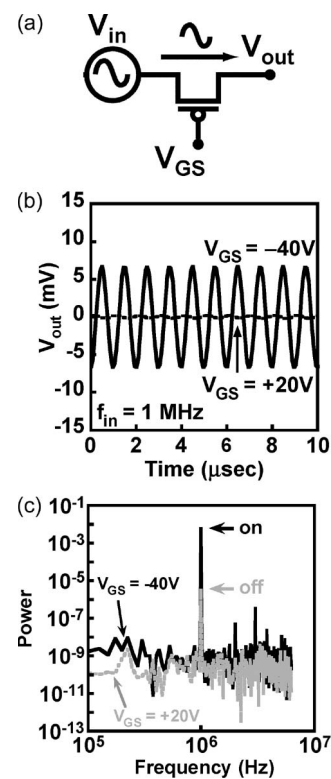

Fig. 6. High-speed printed organic FETs. (a) Measurement circuit of grounded-gate organic transistors. (b) One-megahertz operation of the organic FETs with a grounded gate. (c) Power spectrum of the output waveform shown in (a). A high on/off ratio of 10^3 is obtained at 1 MHz.

the dc characteristics prior to measuring the ac characteristics. The typical dc characteristics of the manufactured transistors are shown in Fig. 5. For an ultrasonic imaging device application, the characteristics in a linear regime are very important for sensing and switching a small signal ($\sim$1 mV) generated from the ultrasonic receivers. As can be seen in Fig. 5(b) and (c), the manufactured transistors exhibit good linear behavior in the small-signal regime, indicating that good ohmic contacts can be obtained in the manufactured organic transistors. This characteristic is very important since the ultrasonic transducers are operated at a very low voltage of $\sim$1 mV$_{p-p}$. The mobility in the saturation regime is 0.5 cm^2/V $\cdot$ s, and the on/off ratio is 10^7 when the off current is defined as a minimum current at the gate bias of $+10$ V in dc measurements.

In the ultrasonic device, the organic transistor active matrix switches the ac signal that is generated at the ultrasonic receivers or applied to the ultrasonic transmitters. In these situations, a dc bias is applied to the gate, whereas an ac signal is applied to the drain. Note that organic transistors have considerably large capacitance coupling between electrodes because of their process limit and structure, and this causes an unintentional signal flow from the source to the drain electrode. This flow is independent of the gate voltage at a high frequency. Fig. 6 shows the output waveform: The ac voltage of 1 V$_{p-p}$

sine wave is applied to the source and the drain by using a function generator, whereas the constant voltage (-40 V for the ON state or $+20$ V for the OFF state) is applied to the gate [Fig. 6(a)]. The output voltage V_{out} at the source is measured using an oscilloscope. Note that the output voltage at the OFF state is large and limits the on/off ratio in the low-frequency regime, even below the cutoff frequency. When the output voltage at the ON and OFF states [Fig. 6(b)] is transformed by a Fourier transformer using a power spectrum, we obtain a good on/off ratio of $> 10^3$ at 1 MHz and $> 10^4$ at 40 kHz [Fig. 6(c)]. The output voltage in the OFF state is mainly due to capacitive coupling between source and drain electrodes.

B. Stand-Alone Ultrasonic Transducer

The stand-alone characteristics of ultrasonic transducers are characterized. A commercial PVDF ultrasonic transducer with a resonance frequency of 40 kHz is used for the transmission of the ultrasonic wave with the application of an input voltage of 200 V$_{p-p}$ using the pulser/receiver. The frequency of the input voltage is 40 kHz. The output waveform from ultrasonic receivers is amplified by 40 dB by the pulser/receiver. The typical received waveform of the manufactured ultrasonic transducers is shown in Fig. 7(a). The manufactured ultrasonic receivers show an output voltage of $\sim$0.8 V$_{p-p}$ after an amplification of 40 dB by the incidence of an ultrasonic wave. The manufactured transducer shows a small Q value of 4 and a narrow pulsewidth of 100 μs, which is suitable for a high-resolution proximity sensor.
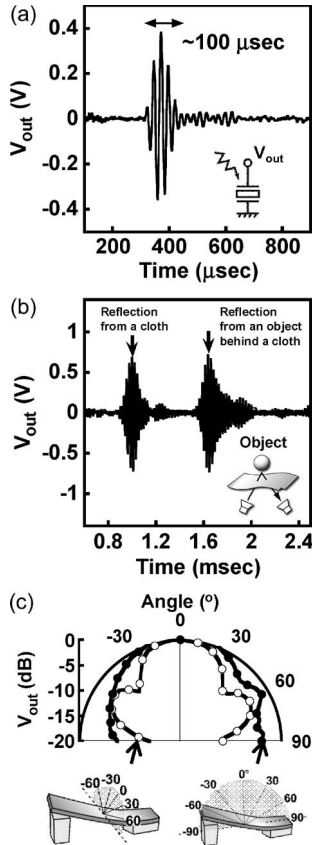
Fig. 7. Stand-alone ultrasonic transducer. (a) Typical waveform V_{out} received at the transducers. The signal is amplified by a 40-dB gain ac amplifier. The frequency of the transmitting signal is 40 kHz. (b) Received waveform reflected from a stiff object behind a cloth. (c) Angular dependence of V_{out}. The ultrasonic transducers can detect signals at an angle of $180°$.

An ultrasonic wave can permeate through a perforated object, which has holes whose dimensions are approximately equal to the wavelength of the ultrasonic wave. We have conducted experiments for detecting an object behind a cloth by using an ultrasonic wave. We place the manufactured ultrasonic transducers in front of a cloth and a reflector behind the cloth. The ultrasonic wave transmitted from the transmitter is reflected on the cloth, whereas a part of the ultrasonic wave goes thorough the cloth and is reflected on the target object behind the cloth. Then, the reflected ultrasonic wave is detected by the ultrasonic receiver. The result is shown in Fig. 7(b). The reflected wave from both the cloth and the target object is shown in the output waveform. The frequency of the proposed ultrasonic device is 40 kHz, which corresponds to the wavelength of 8.5 mm in air. Furthermore, a part of the ultrasonic wave can transmit through a cloth. In our experiment, 60% of the ultrasonic wave permeates through a cloth. The ultrasonic transducers can detect a stiff object that is hidden inside a cloth and which cannot be detected by other imaging devices such as a camera.

Fig. 7(c) shows the directivity of the manufactured ultrasonic receiver. This figure shows a broad directivity, i.e., > -5 dB for an incident angle of $\pm60°$. This broad directivity is suitable for use in a synthetic aperture technique. In the width direction, the receiver shows a symmetrical directivity and peak at $\pm60°$ because of the superposition of the incident ultrasonic wave. In the length direction, it shows an almost symmetrical directivity,
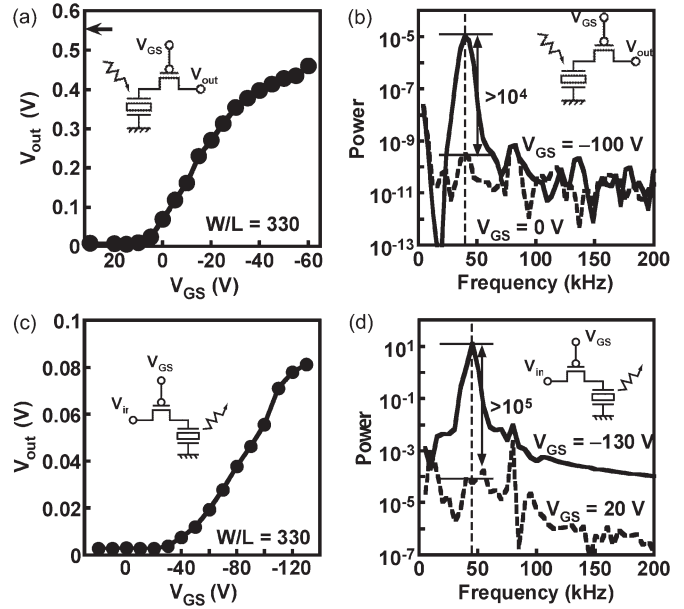

Fig. 8. Ultrasonic sensing cells comprising organic FETs and ultrasonic transducers. (a) Switching characteristics of the ultrasonic cell in the receiver mode with changing V_{GS} of the organic transistor. (b) Power spectrum of the ultrasonic sensing cell for (solid line) $V_{GS} = -100$ V and (dashed line) $V_{GS} = 0$ V. The on/off ratio is $> 10^4$. (c) Switching characteristics of the ultrasonic cell in the transmitter mode. (d) Power spectrum of the ultrasonic transmitter cell for (solid line) $V_{GS} = -130$ V and (dashed line) $V_{GS} = 20$ V. The on/off ratio is $> 10^5$.

but the peak at $60°$ is observed because of the bending structure of the transducers. An almost identical directivity is observed in the case of all the transmitters.

C. Integrated Imaging System

The characteristics of the integrated ultrasonic sensing cell comprising one ultrasonic transducer and one organic FET are investigated. Fig. 8(a) shows the gate voltage dependence of the output voltage of an ultrasonic sensing cell. One of the electrodes of the ultrasonic receiver is connected to the drain of the organic transistor, whereas the other electrode is connected to the ground. The output signal generated at the ultrasonic receiver by the incidence of the ultrasonic wave is controlled by a bias voltage applied to the gate of the organic transistor. The input voltage of 200 V_{p-p} is applied to the transmitter by using a pulser/receiver. The output waveform from the source of the organic transistor is amplified by the pulser/receiver at 50 dB. The output voltage at a gate voltage of -60 V is approximately 89% of that of the stand-alone transducer. The power spectrum of the output wave is shown in Fig. 8(b) for gate voltages of -100 and 0 V. The signal from the ultrasonic transducer is well switched by the organic FET at 40 kHz, and the on/off ratio at 40 kHz is $> 10^4$.

The operation of ultrasonic cells as a transmitter is also investigated. The test circuit is similar to that of the receiver mode. The input signal to the ultrasonic transducer is switched by the gate bias voltage. The gate voltage dependence and its power spectrum are shown in Fig. 8(c) and (d), respectively. The switching of the signal to the ultrasonic transducer can be controlled by the organic FET. The output voltage is approximately 22% smaller than that of stand-alone ultrasonic
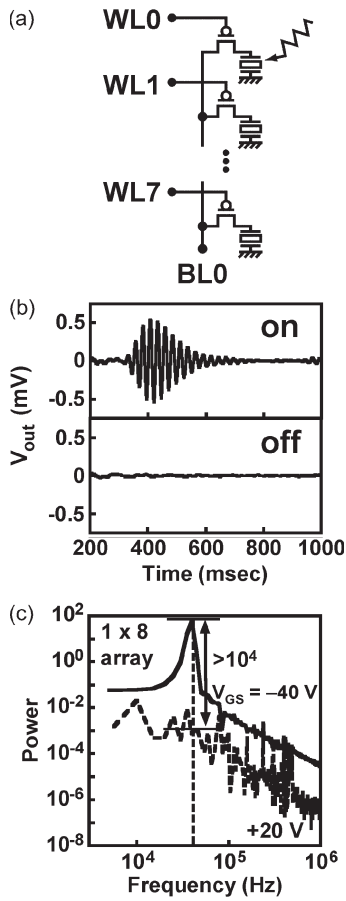
Fig. 9. Crosstalk in the ultrasonic cells linear array. (a) Experimental setup for a crosstalk measurement. The eight sensing cells are connected to each other through the common BL. All the eight cells are used as receiver cells. (b) Output waveforms V_{out} of the ultrasonic sensing cell in the 1×8 ultrasonic sensing array for $V_{GS} = -40$ V (on) and 20 V (off). (c) Power spectrum of the output waveforms shown in (b) for (solid line) $V_{GS} = -40$ V and (dashed line) $V_{GS} = 20$ V. The ultrasonic sensing cell in the 1×8 ultrasonic sensing array also exhibits a sufficient on/off ratio of $> 10^4$.

transducers when the gate voltage is -130 V. In the transmitter mode, an on/off ratio of $> 10^5$ is obtained at 40 kHz. The different characteristic between the receiver and the transmitter is mainly due to both variation in transistor performances and transducer coupling.

Moreover, the crosstalk of the integrated ultrasonic sensing cells is characterized. The eight ultrasonic transducers are connected to the eight transistors that have a common bit line (BL). All the eight cells are used as receiver cells. In this configuration, the integrated ultrasonic sensing cells have a sufficient on/off ratio of 10^4 at 40 kHz when the gate voltage is -40 V for the ON state or 20 V for the OFF state, as shown in Fig. 9.

D. Imaging

An imaging experiment using the ultrasonic sensing array in free space is carried out. The spatial images are obtained by using a synthetic aperture method [25], [26]. The reflected ultrasonic wave from target objects is detected by an array of ultrasonic receivers, and the image of the object is reconstructed. A high-resolution 3-D spatial image can be reconstructed using a 2-D array of ultrasonic receivers. First, the target object whose dimensions are 50 mm $\times$ 50 mm is detected by a 1×8 linear
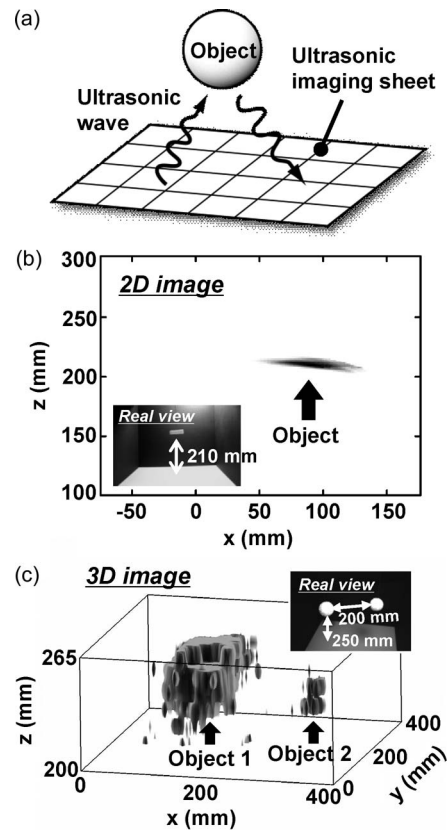

Fig. 10. Ultrasonic imaging. (a) Experimental setup of ultrasonic imaging. A 3-D image of the object can be reconstructed (synthetic aperture method) using all the received signals. (b) 2-D image obtained by a 1×8 ultrasonic sensing array comprising ultrasonic transducers and organic transistors. The x-axis represents the direction of the linear array of ultrasonic sensing cells, and the z-axis represents the direction perpendicular to the linear array. (c) 3-D image obtained by 17×11 stand-alone ultrasonic transducers.

array of ultrasonic sensing cells. The measurement setup and the result are shown in Fig. 10(a). A 2-D image, representing the direction of the linear array of the ultrasonic sensing cells on the x-axis and the direction perpendicular to the linear array on the z-axis, is obtained by the ultrasonic sensor array. In this experiment, all the 1×8 ultrasonic sensing cells are used as receivers, and one PVDF ultrasonic transmitter is used in addition to the linear array. The readout of the reflected waveform is scanned one by one by the organic transistors. Since $>99\%$ of the ultrasonic wave is reflected at the surface of the target object in this case, only the bottom surface of the target object can be detected. A clear image is obtained, as shown in Fig. 10(b). According to the principles of the synthetic aperture technique, the resolution along the z-axis is better than that along the x- and y-axes. However, further improvement will be feasible only if the area or number of receivers and/or transmitters is increased. As shown in Fig. 10(c), a 3-D image is obtained by using the 17×11 two-dimensional stand-alone ultrasonic transducers without organic transistors.

IV. DISCUSSION

Here, we would like to address the advantages of ultrasonic imaging devices in comparison with other imaging devices. In recent times, 3-D sensing of the position of the people and

objects in free space has been carried out by using several methods that are based on visible light, radio waves, millimeter waves, and/or ultrasonic waves. All of these methods have both merits and demerits, and an optimal method that considers target materials, measurement environment, required resolution, distance, and cost is used. Ultrasonic imaging [27]–[30] can offer attractive features such as real-time nondestructive 3-D imaging in free space at an ultralow cost. Ultrasonic waves are now widely used for nondistractive testing [31], fabrication of intervehicular distance sensors [32], and medical ultrasonic imaging [33]. Unlike these applications, the proposed device can detect 3-D spatial information in free space. The resolution of the spatial image obtained by the synthetic aperture method depends on the number, density, and area of the array of ultrasonic receivers. As shown in Fig. 10(b) and (c), a large aperture and a large number of receivers are needed to obtain high-resolution spatial images, particularly along the plane that is parallel to the receiver array. A large-area array of ultrasonic receivers is required to obtain a high-resolution image; however, it is difficult to manufacture a large-area receiver array using PZT or other ceramic piezoelectric material integrated with inorganic electronics at a low cost. In this paper, we realized a large-area ultrasonic imaging sheet compatible with 3-D imaging using a polymer piezoelectric material and an organic transistor active matrix.

In the ultrasonic imaging sheet with an active matrix of organic transistors that switch ac input and/or output signals, it is important to significantly improve the ac characteristics of organic transistors. For this purpose, improvement of mobility and reduction of channel length are crucial. In addition to pentacene, some organic semiconductors are known to exhibit a high mobility value of $> 1 \ cm^2/V \cdot s$ in ambient air such as [1]Benzothieno[3,2-b]benzothiophene derivatives [34] and 6,13-bis(triisopropyl-silylethynyl) pentacene [35]. Furthermore, with an increase in mobility, the frequency response of organic transistors has been improved [36]. It is important not only to improve mobility but also to decrease the channel length for high-frequency operation. Indeed, by reducing the channel length to 0.48 μm, a transition frequency f_T of 2 MHz has been achieved in the case of polymer FETs [37]. Moreover, in the case of logic circuits based on organic transistors, 64-bit code generators for RFID systems [11], complementary D flip-flops [38], and ultralow-power organic complementary ring oscillators that operate at a supply voltage of 1.5 V [39] have been reported. In all these ICs, organic transistors have a source-grounded configuration.

Meanwhile, organic transistors in the ultrasonic device have a gate-grounded configuration; an ac signal from/to ultrasonic transducers is applied to the drain, whereas a constant voltage is applied to the gate. Gate-grounded ac characteristics of organic transistors are as important as the source-grounded ac characteristics in many applications such as active matrices in sensors; however, little attention has been paid to these gate-grounded ac characteristics. In ultrasonic devices, as in the case of organic active matrices that are used for display applications, not only a high cutoff frequency but also a high on/off ratio is required when the number of ultrasonic cells becomes large. Note that organic transistors have a rather large

overlap area and large capacitance coupling between electrodes because they are generally fabricated using a simple mechanics for low-cost registration, as compared with advanced silicon technology. Such capacitance coupling causes an unintentional ac signal that limits the on/off ratio flows from the drain to the source, even in the frequency region below the cutoff frequency. Therefore, reducing capacitance coupling between electrodes is important for obtaining a high on/off ratio with grounded-gate organic transistors.

To decrease the capacitance, we have cut down the width of the source/drain electrodes. Low channel resistance is needed for high sensitivity of the ultrasonic cells; however, the source and drain electrodes that have large channel width cause large parasitic capacitance between electrodes. This capacitance drastically degrades the OFF state of the transistors. In this paper, we have successfully obtained a high on/off ratio of $> 10^4$ with gate-grounded organic transistors, even at an ultrasonic frequency of 40 kHz, by reducing the width of the source and drain electrodes. Furthermore, to reduce the width of electrodes with large-area scalability, inkjet printing technologies with subfemtoliter accuracy have recently been developed [40], [41]. These technologies will drastically improve the ac characteristics of organic transistors.

Another possible method is electrical shielding using an electrically grounded top-gate electrode placed over source/drain electrodes. The capacitive coupling between the source and the drain can be suppressed by electric shielding on source/drain electrodes. By placing the grounded electrode immediately over the source/drain electrode such as the top gate connected to the ground, the electric flux line from the drain to the source is cut by the shielding electrode. Then, the capacitance between the source and the drain decreases. Moreover, in the large-area circuit, the resistance and the capacitance are large because of the interconnections and the circuit layout. In considerably large-area sensors or actuators, suppressing the capacitance between interconnections, such as word lines and BLs, is also very important for obtaining smaller crosstalk between the transistors at a high frequency. If grounded-gate organic transistors can operate at a high frequency of > 1 MHz with a sufficiently high on/off ratio after these improvements, the resolution of the ultrasonic imaging sheet becomes higher; this increase in resolution expands the sheet's scope of application in the field of medicine.

In this paper, the spatial image is obtained by using the synthetic aperture method; however, we can use the ultrasonic transducer matrix as a proximity sensor matrix because each cell of the ultrasonic transducer matrix in the proposed device can be used as both a receiver and a transmitter without any change. Moreover, we do not have to use all transducers every time. We can choose the area and number of transducers that we wish to use according to the measurement area, resolution, and scan rate that we expect.

V. SUMMARY

In this paper, we have successfully fabricated a large-area flexible ultrasonic 3-D imaging system by integrating an array sheet of ultrasonic transducers, which is made of a polymer

piezoelectric material, with an active matrix of printed organic FETs. The printed transistors ($\mu \sim 0.5 \ \mathrm{cm^2/V \cdot s}$) with a grounded gate can switch 40-kHz signals with an on/off ratio of $> 10^4$. The system comprises 8×8 ultrasonic sensing cells or others and has a printed area of $25 \times 25 \ \mathrm{cm^2}$. Three-dimensional ultrasonic images can be obtained for multiple-target objects over this sheet. This system can detect target objects behind a cloth and a paper. It is mechanically flexible and can be wrapped around a cylindrical bar; this configuration is suitable for obtaining a viewing angle of $360°$ for a medium-length (about several meters) proximity robotic skinlike sensor.

ACKNOWLEDGMENT

REFERENCES

[1] S. R. Forrest, "The path to ubiquitous and low-cost organic electronic appliances on plastic," *Nature*, vol. 428, no. 6986, pp. 911–918, Apr. 2004.

[2] G. Horowitz, "Organic thin film transistors: From theory to real devices," *J. Mater. Res.*, vol. 19, no. 7, pp. 1946–1962, Jul. 2004.

[3] H. Sirringhaus, "Device physics of solution-processed organic field-effect transistors," *Adv. Mater.*, vol. 17, no. 20, pp. 2411–2425, Oct. 2005.

[4] H. Klauk, *Organic Electronics: Materials, Manufacturing, and Applications*. Weinheim, Germany: Wiley-VCH, Aug. 2006.

[5] Z. Bao and J. Locklin, *Organic Field-Effect Transistors*. Boca Raton, FL: CRC Press, May 2007.

[6] J. A. Rogers, Z. Bao, K. Baldwin, A. Dodabalapur, B. Crone, V. R. Raju, V. Kuck, H. Katz, K. Amundson, J. Ewing, and P. Drzaic, "Paperlike electronic displays: Large-area rubberstamped plastic sheets of electronics and microencapsulated electrophoretic inks," in *Proc. Nat. Acad. Sci.*, Apr. 2001, vol. 98, no. 9, pp. 4835–4840.

[7] G. H. Gelinck, H. E. A. Huitema, E. Van Veenendaal, E. Cantatore, L. Schrijnemakers, J. B. P. H. Van der Putten, T. C. T. Geuns, M. Beenhakkers, J. B. Giesbers, B. H. Huisman, E. J. Meijer, E. M. Benito, F. J. Touwslager, A. W. Marsman, B. J. E. Van Rens, and D. M. De Leeuw, "Flexible active-matrix displays and shift registers based on solution-processed organic transistors," *Nat. Mater.*, vol. 3, no. 2, pp. 106–110, Feb. 2004.

[8] K. Nomoto, N. Hirai, N. Yoneya, N. Kawashima, M. Noda, M. Wada, and J. Kasahara, "A high-performance short-channel bottom-contact OTFT and its application to AM-TN-LCD," *IEEE Trans. Electron Devices*, vol. 52, no. 7, pp. 1519–1526, Jul. 2005.

[9] P. F. Baude, D. A. Ender, M. A. Haase, T. W. Kelley, D. V. Muyres, and S. D. Theiss, "Pentacene-based radio-frequency identification circuitry," *Appl. Phys. Lett.*, vol. 82, no. 22, pp. 3964–3966, Jun. 2003.

[10] R. Rotzoll, S. Mohapatra, V. Olariu, R. Wenz, M. Grigas, K. Dimmler, O. Shchekin, and A. Dodabalapur, "Radio frequency rectifiers based on organic thin-film transistors," *Appl. Phys. Lett.*, vol. 88, no. 12, p. 123 502, Mar. 2006.

[11] E. Cantatore, T. C. T. Geuns, G. H. Gelinck, E. van Veenendaal, A. F. A. Gruijthuijsen, L. Schrijnemakers, S. Drews, and D. M. de Leeuw, "A 13.56-MHz RFID system based on organic transponders," *IEEE J. Solid-State Circuits*, vol. 42, no. 1, pp. 84–92, Jan. 2007.

[12] J. B. Chang, V. Liu, V. Subramanian, K. Sivula, C. Luscombe, A. Murphy, J. S. Liu, and J. M. J. Frechet, "Printable polythiophene gas sensor array for low-cost electronic noses," *J. Appl. Phys.*, vol. 100, no. 1, p. 014506, Jul. 2006.

[13] M. C. Tanes, D. Fine, A. Dodabalapur, and L. Torsi, "Organic thin-film transistor sensors: Interface dependent and gate bias enhanced responses," *Microelectron. J.*, vol. 37, no. 8, pp. 837–840, Aug. 2006.

[14] T. Someya, Y. Kato, T. Sekitani, S. Iba, Y. Noguchi, Y. Murase, H. Kawaguchi, and T. Sakurai, "Conformable, flexible, large-area networks of pressure and thermal sensors with organic transistor active matrixes," in *Proc. Nat. Acad. Sci.*, Aug. 2005, vol. 102, no. 35, pp. 12 321–12 325.

[15] T. Someya, T. Sekitani, S. Iba, Y. Kato, H. Kawaguchi, and T. Sakurai, "A large-area, flexible pressure sensor matrix with organic field-effect

[16] transistors for artificial skin applications," in *Proc. Nat. Acad. Sci.*, Jul. 2004, vol. 101, no. 27, pp. 9966–9970.

[16] T. Someya, Y. Kato, S. Iba, H. Kawaguchi, and T. Sakurai, "Integration of organic field-effect transistors with organic photodiodes for a large area, flexible, and lightweight sheet image scanner," *IEEE Trans. Electron Devices*, vol. 52, no. 11, pp. 2502–2511, Nov. 2005.

[17] Y. Kato, T. Sekitani, M. Takamiya, M. Doi, K. Asaka, T. Sakurai, and T. Someya, "Sheet-type Braille displays by integrating organic field-effect transistors and polymeric actuators," *IEEE Trans. Electron Devices*, vol. 54, no. 2, pp. 202–209, Feb. 2007.

[18] T. Sekitani, M. Takamiya, Y. Noguchi, S. Nakano, Y. Kato, T. Sakurai, and T. Someya, "A large-area wireless power-transmission sheet using printed organic transistors and plastic MEMS switches," *Nat. Mater.*, vol. 6, no. 6, pp. 413–417, Jun. 2007.

[19] T. Sekitani, Y. Noguchi, S. Nakano, K. Zaitsu, Y. Kato, M. Takamiya, T. Sakurai, and T. Someya, "Communication sheets using printed organic nonvolatile memories," in *IEDM Tech. Dig.*, Dec. 2007, pp. 221–225.

[20] Y. Kato, T. Sekitani, Y. Noguchi, M. Takamiya, T. Sakurai, and T. Someya, "A large-area, flexible, ultrasonic imaging system with a printed organic transistor active matrix," in *IEDM Tech. Dig.*, Dec. 2008, pp. 97–100.

[21] Y. Noguchi, T. Sekitani, T. Yokota, and T. Someya, "Direct inkjet printing of silver electrodes on organic semiconductors for thin-film transistors with top contact geometry," *Appl. Phys. Lett.*, vol. 93, no. 4, p. 043 303, Jul. 2008.

[22] Y. Noguchi, T. Sekitani, and T. Someya, "Printed shadow masks for organic transistors," *Appl. Phys. Lett.*, vol. 91, no. 13, p. 133 502, Sep. 2007.

[23] A. S. Fiorillo, "Design and characterization of a PVDF ultrasonic range sensors," *IEEE Trans. Ultrason., Ferroelectr., Freq. Control*, vol. 39, no. 6, pp. 688–692, Nov. 1992.

[24] M. Toda and S. Tosima, "Theory of curved, clamped, piezoelectric film, air-borne transducers," *IEEE Trans. Ultrason., Ferroelectr., Freq. Control*, vol. 47, no. 6, pp. 1421–1431, Nov. 2000.

[25] J. T. Ylitalo and H. Ermert, "Ultrasound synthetic aperture imaging: Monostatic approach," *IEEE Trans. Ultrason., Ferroelectr., Freq. Control*, vol. 41, no. 3, pp. 333–339, May 1994.

[26] G. R. Lockwood, J. R. Talman, and S. S. Brunke, "Real-time 3-D ultrasound imaging using sparse synthetic aperture beamforming," *IEEE Trans. Ultrason., Ferroelectr., Freq. Control*, vol. 45, no. 4, pp. 980–988, Jul. 1998.

[27] E. D. Light, R. E. Davidsen, J. O. Fiering, T. A. Hruschka, and S. W. Smith, "Progress in 2-D arrays for real time volumetric imaging," *Ultrason. Imaging*, vol. 20, no. 1, pp. 1–15, Jan. 1998.

[28] S. W. Smith, H. G. Pavy, Jr., and O. T. von Ramm, "High-speed ultrasound volumetric imaging system—Part I: Transducer design and beam steering," *IEEE Trans. Ultrason., Ferroelectr., Freq. Control*, vol. 38, no. 2, pp. 100–108, Mar. 1991.

[29] A. Austeng and S. Holm, "Sparse 2-D arrays for 3-D phased array imaging—Design methods," *IEEE Trans. Ultrason., Ferroelectr., Freq. Control*, vol. 49, no. 8, pp. 1073–1086, Aug. 2002.

[30] S. W. Smith, K. Chu, S. F. Idriss, N. M. Ivancevich, E. D. Light, and P. D. Wolf, "Feasibility study: Real-time 3-D ultrasound imaging of the brain," *Ultrasound Med. Biol.*, vol. 30, no. 10, pp. 1365–1371, Oct. 2004.

[31] B. W. Drinkwater and P. D. Wilcox, "Ultrasonic arrays for non-destructive evaluation: A review," *NDT E Int.*, vol. 39, no. 7, pp. 525–541, Oct. 2006.

[32] W. S. H. Munro, S. Pomeroy, M. Rafiq, H. R. Williams, M. D. Wybrow, and C. Wykes, "Ultrasonic vehicle guidance transducer," *Ultrasonics*, vol. 28, no. 6, pp. 350–354, Nov. 1990.

[33] S. W. Smith, G. E. Trahey, and O. T. von Ramm, "Two-dimensional arrays for medical ultrasound," *Ultrason. Imaging*, vol. 14, no. 3, pp. 213–233, Jul. 1992.

[34] H. Ebata, T. Izawa, E. Miyazaki, K. Takimiya, M. Ikeda, H. Kuwabara, and T. Yui, "Highly soluble [1]Benzothieno[3,2-b]benzothiophene (BTBT) Derivatives for high-performance, solution-processed organic field-effect transistors," *J. Amer. Chem. Soc.*, vol. 129, no. 51, pp. 15 732–15 733, Dec. 2007.

[35] S. K. Park, T. N. Jackson, J. E. Anthony, and D. A. Mourey, "High mobility solution processed 6,13-bis(triisopropyl-silylethynyl) pentacene organic thin film transistors," *Appl. Phys. Lett.*, vol. 91, no. 6, p. 063514, Aug. 2007.

[36] S. K. Park, J. E. Anthony, and T. N. Jackson, "Solution-processed TIPS-pentacene organic thin-film-transistor circuits," *IEEE Electron Device Lett.*, vol. 28, no. 10, pp. 877–879, Oct. 2007.

[37] V. Wagner, P. Wöbkenberg, A. Hoppe, and J. Seekamp, "Megahertz operation of organic field-effect transistors based on poly(3-hexylthiopene)," *Appl. Phys. Lett.*, vol. 89, no. 24, p. 243 515, Dec. 2006.

[38] B. Yoo, A. Madgavkar, B. A. Jones, S. Nadkarni, A. Facchetti, K. Dimmler, M. R. Wasielewski, T. J. Marks, and A. Dodabalapur, "Organic complementary D flip-flops enabled by perylene diimides and pentacene," *IEEE Electron Device Lett.*, vol. 27, no. 9, pp. 737–739, Sep. 2006.

[39] H. Klauk, U. Zschieschang, J. Pflaum, and M. Halik, "Ultralow-power organic complementary circuits," *Nature*, vol. 445, no. 7129, pp. 745–748, Feb. 2007.

[40] J. Park, M. Hardy, S. J. Kang, K. Barton, K. Adair, D. K. Mukhopadhyay, C. Y. Lee, M. S. Strano, A. G. Alleyne, J. G. Georgiadis, P. M. Ferreira, and J. A. Rogers, "High-resolution electrohydrodynamic jet printing," *Nat. Mater.*, vol. 6, no. 10, pp. 782–789, Oct. 2007.

[41] T. Sekitani, Y. Noguchi, U. Zschieschang, H. Klauk, and T. Someya, "Organic transistors manufactured using inkjet technology with sub-femtoliter accuracy," in *Proc. Nat. Acad. Sci.*, Apr. 2008, vol. 105, no. 13, pp. 4976–4980.

Yusaku Kato (S'05) was born in Tokyo, Japan, in 1981. He received the B.S. and Ph.D. degrees in applied physics from The University of Tokyo, Tokyo, in 2004 and 2009, respectively.

He is currently with Sony Corporation, Tokyo.

Tsuyoshi Sekitani received the B.S. degree from Osaka University, Suita, Japan, in 1999 and the Ph.D. degree in applied physics from The University of Tokyo, Tokyo, Japan, in 2003.

From 1999 to 2003, he was with the Institute for Solid State Physics, The University of Tokyo. From 2003 to 2009, he was a Research Associate with the Quantum-Phase Electronics Center, School of Engineering, The University of Tokyo. Since 2009, he has been a Research Associate with the Department of Electrical and Electronic Engineering, The University of Tokyo.
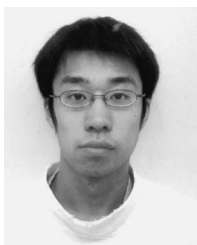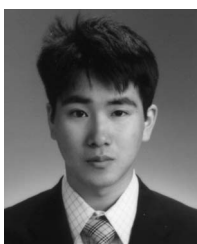
Yoshiaki Noguchi was born in Kanagawa, Japan, in 1983. He received the M.S. degree in applied physics in 2007 from The University of Tokyo, Tokyo, Japan, where he is currently working toward the Ph.D. degree in applied physics.

His research interests include organic transistors, large-area electronics, and printed electrical devices.

Mr. Noguchi is a Student Member of the Japanese Society of Applied Physics and a member of the Japan Society for the Promotion of Science Research Fellowships.

Tomoyuki Yokota was born in Tokyo, Japan, in 1985. He received the B.S. degree in applied physics in 2008 from The University of Tokyo, Tokyo, where he is currently working toward the M.S. degree in applied physics.

His research interests include printed electrical devices, large-area electronics, organic memories, and organic transistors.

Mr. Yokota is a Student Member of the Japanese Society of Applied Physics.

Makoto Takamiya (S'98–M'00) received the B.S., M.S., and Ph.D. degrees from The University of Tokyo, Tokyo, Japan, in 1995, 1997, and 2000, respectively, all in electronic engineering.

In 2000, he joined NEC Corporation, Tokyo, where he was engaged in the circuit design of high-speed digital LSIs and developed the field of on-chip measurement macros to solve the power integrity issues. In 2005, he joined The University of Tokyo, where he is currently an Associate Professor with the VLSI Design and Education Center. His research interests include power and signal integrity issues in LSIs, low-power RF integrated circuits, low-power digital circuits, and large-area electronics with organic transistors.

Takayasu Sakurai (S'77–M'78–SM'01–F'03) received the Ph.D. degree in electrical engineering from The University of Tokyo, Tokyo, Japan, in 1981.

In 1981, he joined Toshiba Corporation, where he designed CMOS DRAM, SRAM, RISC processors, DSPs, and SoC solutions. He has extensively worked on interconnect delay and capacitance modeling known as Sakurai model and alpha-power-law MOS model. From 1988 to 1990, he was a Visiting Researcher with the University of California, Berkeley, where he conducted research in the field of VLSI CAD. Since 1996, he has been a Professor with The University of Tokyo, working on low-power high-speed VLSI, memory design, interconnects, and wireless systems. He is also a consultant to U.S. startup companies. He has published more than 400 technical papers, including 70 invited papers and several books, and has filed more than 100 patents.

Prof. Sakurai served as a Conference Chair for the IEEE/JSAP Symposium on VLSI Circuits and IEEE International Conference on IC Design and Technology, a Vice Chair for the ACM/IEEE Asia and South Pacific Design Automation Conference, and a Program Committee Member for the IEEE International Solid-State Circuits Conference, IEEE Custom Integrated Circuits Conference, ACM/IEEE Design Automation Conference, ACM/IEEE International Conference on Computer-Aided Design, ACM Workshop on Field-Programmable Gate Arrays, ACM/IEEE International Symposium on Low-Power Electronics and Design, ACM/IEEE International Workshop on Timing Issues, and other international conferences. He was a Plenary Speaker for the 2003 IEEE International Solid-State Circuits Conference. He is an elected AdCom Member for the IEEE Solid-State Circuits Society and an IEEE Circuits and Systems Society Distinguished Lecturer.

Takao Someya (M'03) received the Ph.D. degree in electrical engineering from The University of Tokyo, Tokyo, Japan, in 1997.

In 1997, he joined the Institute of Industrial Science, The University of Tokyo, as a Research Associate. He was appointed to be a Lecturer with the Research Center for Advanced Science and Technology (RCAST), The University of Tokyo, in 1998 and an Associate Professor of RCAST in 2002. From 2001 to 2003, he was a Visiting Scholar with the Nanocenter (NSEC), Columbia University, New York, NY, and Bell Laboratories, Lucent Technologies. From 2003 to 2009, he was an Associate Professor with the Department of Applied Physics and Quantum-Phase Electronics Center, School of Engineering, The University of Tokyo. Since 2009, he has been a Professor of electrical and electronic engineering with The University of Tokyo. His current research interests include organic transistors, flexible electronics, plastic integrated circuits, large-area sensors, and plastic actuators.

Prof. Someya has been a Board of Directors of the Materials Research Society since 2009; a Distinguished Lecturer of the IEEE Electron Devices Society since 2004; an International Academic Member at NSEC, Columbia University, since 2003; and a Global Scholar of Princeton University, Princeton, NJ, since 2009. He was the recipient of numerous awards, including the IEEE/ISSCC Sugano Award in 2005, the Marubun Award in 2006, the Japan Society for the Promotion of Science Award in 2008, and the Japan IBM Science Award in 2009.